Available online at www.sciencedirect.com

ScienceDirect

journal homepage: www.elsevier.com/locate/issn/15375110

Research Paper

Performance analysis of a tractor - power harrow system under different working conditions

P. Balsari [a], A. Biglia [a,*], L. Comba [a,b], D. Sacco [a], L. Eloi Alcatrão [a], M. Varani [c], M. Mattetti [c], P. Barge [a], C. Tortia [a], M. Manzone [a], P. Gay [a,1], D. Ricauda Aimonino [a]

[a] Department of Agricultural, Forest and Food Sciences (DiSAFA) – Università degli Studi di Torino, Largo Paolo Braccini 2, 10095, Grugliasco, TO, Italy

[b] CNR-IEIIT – Politecnico di Torino, Corso Duca degli Abruzzi 24, 10129, Torino, Italy

[c] Department of Agricultural and Food Sciences (DiSTAL) – Università degli Studi di Bologna, Viale Giuseppe Fanin 50, 40127, Bologna, Italy

ARTICLE INFO

Article history:
Received 7 August 2020
Received in revised form
16 November 2020
Accepted 24 November 2020
Published online 13 December 2020

Keywords:
Tillage operations
Power Take-Off torque
Draught
Fuel consumption
Energy consumption

Tillage is one of the most important operations in the preparation of land for growing crops. Among secondary tillage implements, power harrows, which have a series of PTO-driven rotors which rotate about their vertical axis, are widely adopted in soil-working operations. Typically, this kind of implement is highly energy consuming, due to the heavy mechanical loads required to pull the harrow and the PTO (Power Take-Off) torque needed to drive the rotors.

This paper reports the results of extensive in-field experimentation in which the relationship between the operating conditions of a tractor - power harrow system and the mechanical loads (i.e. PTO torque and draught) were investigated in two different test site fields. The test parameters consisted of: nominal tractor speed (3, 6, 9 and 12 km h^{-1}), nominal working depth (6, 9 and 15 cm) and rotor speed (285 and 411 rpm) at a PTO speed of 1000 rpm. The data was statistically analysed by means of a linear mixed effect model to assess the differences in the tractor - harrow system performances measured under different working conditions. The presented results show which operating conditions can be favourable regarding energy and fuel consumption as this information may be very useful to farmers to reduce costs. Moreover, the measured mechanical loads concerning PTO torque and draught may also be beneficial for manufacturers to improve the design of these kinds of implements.

* *Corresponding author.*
E-mail address: alessandro.biglia@unito.it (A. Biglia).
[1] Co-last author.

https://doi.org/10.1016/j.biosystemseng.2020.11.009

1. Introduction

Tillage has been performed since ancient times as it is one of the most important stages in the cultivation of agricultural crops; it is defined as the mechanical manipulation of the topsoil (Krause, Lorenz, & Hoogmoed, 1984). The main objectives of tillage are to perform weed control, to incorporate plant residues (Nafi et al., 2020) and organic manure (Garcia-Franco, Albaladejo, Almagro, & Martínez-Mena, 2015), to improve soil moisture (Acharya et al., 2019) and soil tilth (Schjønning & Rasmussen, 2000). Soil tillage has also been recognised as one of the operations that requires high energy and managements costs, such as the need for high power tractors which involves high fuel consumption (Damanauskas, Velykis, & Satkus, 2019; Čiplienė, Gurevičius, Janulevičius, & Damanauskas, 2019). The economic and environmental sustainability of tillage operations is thus mandatory in modern farming (Calcante & Oberti, 2019).

Several studies have focused on the physical and mechanical properties of tilled soil aggregates in order to define which parameters influence the germination and emergence of crops the most (Tagar et al., 2020). In order to obtain uniform and healthy crops with a minimal environmental impact, homogenous aggregate sizes should be obtained over the field (Håkansson, Myrbeck, & Etana, 2002). Indeed, seedbed nutrients and water availability are mostly affected by soil particles distribution while shoot and root growth mainly depends on bulk density (Braunack & Dexter, 1989).

Primary tillage tools such as ploughs, chisels or rippers are widely used, but they do not produce an adequately smooth and fragmented topsoil. Indeed, it has been demonstrated that a good seedbed for cereals should have approximately 50% of the aggregates by weight in the range 0.5–6.0 mm (Berntsen & Berre, 2002). Håkansson et al. (2002) claimed that a limit of more than 50% of aggregates with a diameter of less than 5 mm in the seedbed is required to achieve a rapid and uniform emergence of small grains in different soil textures, even in dry condition. Authors such as Braunack (1995) reported that higher and earlier emergence (under irrigation in clay soil) was found in laboratory seedbeds which consisted of 1–2 mm and 2–5 mm aggregates for soybean and maize, respectively. However, good emergence of soybeans was also observed with coarser aggregates (5–15 mm) due to less drying than in seedbeds with a greater soil pulverisation. Dürr and Aubertot (2000) studied the effects of large aggregates within the seedbed on the emergence of sugar beet seedling in laboratory conditions. They found a decrease in the emergence percentage with aggregates sizes of over 10 mm when these were included within seedbeds consisting of <5 mm sieved soil. In order to obtain such soil aggregates and a smoother topsoil surface, primary tillage is usually followed by secondary tillage (Kayad, Rainato, Picco, Sartori, & Marinello, 2019). Secondary tillage implements are generally towed by agricultural tractors and they can be divided into two main categories: passive and active implements. Passive implements such as disc harrows or vibro-cultivators perform soil fragmentation by absorbing only the tractor drawbar power while active implements also absorb its rotational power since they are actuated by the tractor Power Take-Off (PTO) (Aday, 2015; Navalade, Salokhe, Niyamapa, & Soni, 2010). It has been shown that active and passive secondary tillage implements have similar fragmentation efficiencies even though rotary implements are more effective in the conversion of energy to fragmentation (Adam & Erbach, 1992; Berntsen & Berre, 2002).

Regarding rotary implements, currently, the most widely used ones are rotary tillers and power harrows. The latter were developed more recently, and the main difference with rotary tillers consists in the rotation axis of their blades which is vertical instead of horizontal. Power harrows are widely used because they avoid the formation of tillage pan, facilitate drainage, and may be used at higher forward speeds.

Draught (draft or drawbar pull) can be defined as the force required to pull an implement in the same direction of travel as the tractor. Draught mainly depends upon the working width of the implement and the speed at which the implement is pulled. Moreover, draught is also a function of soil working depth, soil type (e.g. texture, organic matter, etc.), soil conditions (e.g. moisture content) and implement mass (Serrano, Peça, Marques da Silva, Pinheiro, & Carvalho, 2007). Several authors have analysed the effects of varying the working parameters of the implement, such as tractor speed, soil working depth, disc geometry, etc. (Kogut, Sergiel, & Żurek, 2016; Upadhyay & Raheman, 2018) on power needs and tractor fuel consumption (Sahu & Raheman, 2006; Upadhyay & Raheman, 2019, 2020; Usaborisut & Prasertkan, 2018, 2019; Kursat Celik, Caglayan, Topakci, Rennie, & Akinci, 2020).

Nowadays, the topic of energy conversion and mechanical efficiency is very important as most implement manufacturers are focusing on the efficiency increments of their products by designing new optimised shapes and innovative materials to reduce fuel consumption and wear (Mattetti, Varani, Molari, & Morelli, 2017). Therefore, many mathematical models have been focusing on the rotary implements' kinematic and dynamic aspects, in particular on implement travel speed and tine rotational speed (Raparelli, Pepe, Ivanov, & Eula, 2020). The cycloidal movement developed by the tines, both for rotary tillers (Hendrick, 1969; Hendrick & Gill, 1978; Perdok & Kouwenhoven, 1994) and power harrows (Kinzel, Holmes, & Huber, 1981; Perdok & Van de Werken, 1983), has been correlated to soil fragmentation efficiency by performing experimental tests. The results showed that soil fragmentation was strictly correlated to the shape of the developed cycloids for both implements (Chan, Wood, & Holmes, 1993; Destain & Houmy, 1990; Matin, Fielke, & Desbiolles, 2014). Moreover, tillage operations which use rotary implements are typically highly energy consuming due to the draught and the PTO power required for the preparation of the seedbed (Sijtsma, Campbell, McLaughlin, & Carter, 1998). PTO-driven implements, in particular rotary tillers, have been modelled by many authors in order to predict draught power, PTO power absorption and fuel consumption (ASABE Standards, 2006; Grisso, Vaughan, & Roberson, 2008; Ahmadi, 2017), but these models have to be experimentally validated since the interaction between tillage tools and soil is quite complex due to soil heterogeneity and the peculiar process of soil fragmentation (Grisso, Yasin, & Kocher, 1996). Regarding rotary tillers, in-field tests have been performed in different conditions and the

major performance parameters such as draught, tractor speed, PTO torque and rotational speed have been acquired (Kheiralla, Yahya, Zohadie, & Ishak, 2004), while few in-depth experimental tests have been performed for power harrows (Usaborisut & Prasertkan, 2018).

Over the past years, there have been several in-field harrow performance tests during tillage. However, most in-field tillage operations were done using disc harrows at limited forward tractor speeds (generally less than 6 km h^{-1}), while few tillage operations which use power harrows have been tested. Therefore, there has been no recent assessment of PTO, draught power and fuel consumption simultaneously by using a power harrow in different types of soil at forward tractor speeds higher than 6 km h^{-1}. The increment of work productivity is a key factor in modern farming, because farmers have to perform crop operations on large areas in reduced periods of time. This aspect is particularly critical for tillage, as it is mostly carried out in seasons (spring and autumn) with very variable weather conditions. Furthermore, climate change is exacerbating climatic variability (e.g. seasonal temperatures or precipitation patterns), therefore tillage has to be performed quickly in order to exploit favourable conditions, such as rain falls after sowing.

In many cases, farmers would like to couple a power tiller and a seeder to perform seedbed preparation and seeding in one single pass. These aspects lead to the needs to operate the power tiller at ever higher tractor speeds (nowadays, the speed target for seeders is faster than 12 km h^{-1}) with consequent heavier operating conditions, which require implements that are able to withstand high mechanical stress.

This work presents the results of an extensive experimental analysis planned to investigate the relationship between operating conditions and measured forces and energies. In particular, this work provides data for PTO torque and speed, as well as for draught and fuel consumption during secondary tillage operations in two different site test fields by using a 3 m working width power harrow at different working conditions in terms of tractor speed (up to 12 km h^{-1}), working depth and harrow rotors rotational speed.

2. Materials and methods

2.1. Tractor - power harrow system

In-field tests were conducted with a 3 m working width power harrow (Frandent Eternum R303-19, Frandent Group Srl, Italy) equipped with a packer roller. The speed of the harrow rotors can be modified by substituting a couple of cog wheels within the harrow gear box, while keeping the PTO speed constant. Twelve different working depths (up to 22 cm) can be set by changing the inclination of the roller by acting on a couple of pins. The theoretical working depth is given by the distance between the roller surface and the tip of the tines. The specifications of the power harrow are reported in Table 1.

The power harrow was pulled by a four-wheel-drive row crop tractor (Fendt 718 Vario, AGCO GmbH, Germany) with a 132 kW maximum engine power and an unladen mass of 7155 kg (OECD, 2010). A ballast of about 1200 kg was hooked to the front three-point hitch to reduce wheel slippage. Tyre pressure was within the range recommended by the manufacturer (OECD, 2010). The tractor was turned on at the minimum regime one hour before the in-field tests and engaging its rear PTO in order to warm up the tractor fluids and the harrow lubricants.

Table 1 – Specifications of the power harrow used in the field tests.

Working width [m]	3
Number of rotors	12
Rotor tine length [mm]	290
Roller diameter [mm]	550
Mass (harrow + roller) [kg]	1323
Rotor speed at 1000 rpm PTO speed [rpm]	285[a] - 341–411[a]

[a] Speeds considered in the experimental campaigns.

2.2. Sensors and data acquisition system

A three-point hitch coupler, equipped with three biaxial load pins, was installed between the tractor and the power harrow to measure the draught force (Kursat Celik et al., 2020; Mattetti et al., 2017). Biaxial load pins (N.B.C. Elettronica Group Srl, Italy) were able to take over the force along two orthogonal axes (horizontal and vertical) with a load capacity of 10 kN along each direction.

The torque absorbed by the power harrow and the PTO speed were measured by a torque meter (NTCE 7000 series, NTCE AG, Germany) equipped with a factory installed encoder, while the main tractor parameters, as well as the tractor speed, were logged through its Controlled Area Network (CAN) SAE J1939 diagnostic port (Pitla, Luck, Werner, Lin, & Shearer, 2016). Signals with the following Suspect Parameter Numbers (SPNs) and Parameter Group Numbers (PGNs) (SAE, 2013) were considered for the analysis: "Engine Fuel Rate" (SPN 183 - PGN 65266), which reports the amount of fuel consumed by the engine per unit of time, denoted as fuel rate in the following, and "Front Axle Speed" (SPN 904 - PGN 65215), which gives the average speed of the two front wheels.

An embedded data acquisition system was developed by adopting an NI cDAQ-9132 platform (National Instruments, USA) equipped with: (i) an NI 9220 analog input module (16 channels, maximum rate 100 KS s^{-1} per channel, 16 bit) for the acquisition of torque and load pins signals (ii) an NI 9411 digital input module for tachometer signals, as PTO speed, and (iii) a single port high speed CAN module (NI 9862).

A LabVIEW® (National Instruments, USA) application was developed to manage the data acquisition process. Analog signals from the torque meter and the load pins were logged at the sampling rate of 1 kHz, while PTO speed and CAN messages were recorded every 100 ms, generating two separate storage TDMS files. The CAN data was converted into engineering units through the SAE J1939 database (SAE, 2013), directly managed by the LabVIEW® XML library prior to being recorded.

The data acquisition system during tillage operations was set to record: (i) PTO torque [Nm] and its speed [rpm], (ii) tractor speed [km h^{-1}], (iii) fuel rate [l h^{-1}], and (iv) the forces measured by the three load pins [kN] to determine the draught.

2.3. Experimental sites and soil characteristics

The research was carried out over the 2019 season in a farm (site A) located in Poirino (N 44°55′ and E 7°51′) and in the experimental farm (site B) of the University of Turin located in Carmagnola (N 44°51′ and E 7°43'). Both sites are in the Piedmont Region, in north-western Italy. The climate is classified as Humid Subtropical (Cfa) according to the Köppen-Geiger climate classification (Köppen, 1936) and is characterised by hot summers and two main rainy periods in spring and autumn. Trials were carried out between March and April 2019. The test site fields were ploughed in autumn 2018 at about 30 cm depth to incorporate plant residues.

To describe the soil properties of the two sites before harrowing, a soil survey was performed on samples collected at the beginning of the experiment. The soil samples were randomly collected in nine different locations within each test site to determine soil texture, average bulk density, and average water content. Soil penetration resistance and soil cohesion were also determined within the nine sampling points. Soil texture was assessed by the pipette method (Gee & Bauder, 1986) after Na-hexametaphosphate dispersion, adopting the USDA textural soil classification (USDA and NRCS, 2012). Soil penetration resistance was measured through a 30° cone angle hand-held penetrometer (Field Scout SC-900, Spectrum Technologies Inc., USA) following ASABE standards EP 542 (2018), while a shear vane (90 mm high, 45 mm in diameter, measurements at about 3–12 cm depth) was used to quantify soil cohesion (shear strength) in accordance with Arvidsson, Keller, and Gustafsson (2004). The soil properties of the experimental fields are reported in Table 2.

After harrowing, a trench was dug orthogonally to the tractor forward direction, in the centre of each parcel, to evaluate the achieved working depth and to collect samples for aggregates size distribution analysis. The achieved working depth was evaluated by removing the layer of loosened soil and by measuring the distance between soil surface and firm base. In each parcel, about 15 kg of tilled soil were collected to determine aggregate size distribution. Soil samples were sieved by following the ASTM C136/C136M (2019) procedures. The percentage in weight of the aggregates, with a diameter of less than 10 mm, was considered as an index to quantify the effect of the working conditions, in particular the forward speed, on the seedbed after harrowing. The value of 10 mm was chosen after considering the literature data (see Introduction) about optimal seedbed conditions, in terms of cloddiness, for seeds germination related to different crops.

Table 2 – Soil properties of the two experimental sites.

Soil composition	Site A	Site B
Sand [kg kg^{-1}100]	34	36
Silt [kg kg^{-1}100]	51	57
Clay [kg kg^{-1} 100]	15	6
Soil texture class	Silt loam	Silt loam
Plastic limit [% by mass]	26	33
Liquid limit [% by mass]	33	40
Soil shear strength [kPa] at the depth of 3–12 cm	31.4	26.7
Dry bulk density [kg m^{-3}] at the depth of 0–15 cm	1260	1300
Water content [g g^{-1}100] at the depth of 0–5 cm	8.3	10.5
Water content [g g^{-1}100] at the depth of 5–10 cm	15.0	17.4
Water content [g g^{-1}100] at the depth of 10–15 cm	16.2	17.9

2.4. Test conditions and experimental design

The experimental design consists in a split-split-plot 2 × 3 × 3 factorial arrangement representing the different operating conditions: (i) two harrow rotor speeds (285 and 411 rpm) at a PTO speed of 1000 rpm; (ii) three nominal working depths (6, 9 and 15 cm), and (iii) three tractor speeds (3, 6 and 9 km h^{-1}). Tillage depth was kept constant by disabling the three-point hitch draught control, avoiding undesired vertical displacements of the implement. Tractor cruise control was used in order to keep the tractor travel speed constant at the tested values during operations.

The two experimental sites were divided into three blocks (24 × 120 m) as three replicates were done per each combination of the tested operating conditions (Fig. 1). Then, each block was divided into two plots (12 × 120 m) where rotor speed was kept constant. Within each plot, 3 sub-plots (4 × 120 m) were further established to test three working depths of the rotor tines and, in each sub-plot, three tractor speeds were also tested over 40 m length parcels (Fig. 1). Therefore, the total number of parcels for each site accounted for 54.

The plots of the experimental trials relating to rotor speeds were not assigned randomly due to the time required to change harrow gearbox cogs, while the sub-plots relating to working depths and tractor speeds were assigned randomly.

Twelve extra parcels of 60 m in length were used to test the tractor - harrow system at a tractor speed of 12 km h^{-1}. Since the tractor engine was not able to supply enough power to pull the harrow at 12 km h^{-1} when operating at a depth of 15 cm, the monitored data was not included in the statistical analysis as the dataset was incomplete.

The volume and surface of the tilled soil varied during the experiments, due to the different working conditions, and this may have affected the torque and draught values. Therefore, the data was also processed to obtain the amount of power (PTO torque multiplied by its speed and draught multiplied by the tractor speed) and energy (power multiplied by working time) needed per tilled soil volume unit and per surface unit. The tilled soil volume and surface were evaluated by considering the central part of each parcel (20 m, see Fig. 1). The data collected in the first and last ten metres of each parcel was eliminated as the tractor speed, when the cruise control was set to 9 km h^{-1}, was not constant (acceleration and deceleration phases of the tractor). Then, the working time taken to till the 20 m of the parcels, which varied according to the tractor speed, was used to evaluate the energy values.

2.5. Statistical analysis

The acquired data was pre-processed to ensure that only reliable values were included in the statistical analysis. Since the data was acquired at different sampling rates and stored

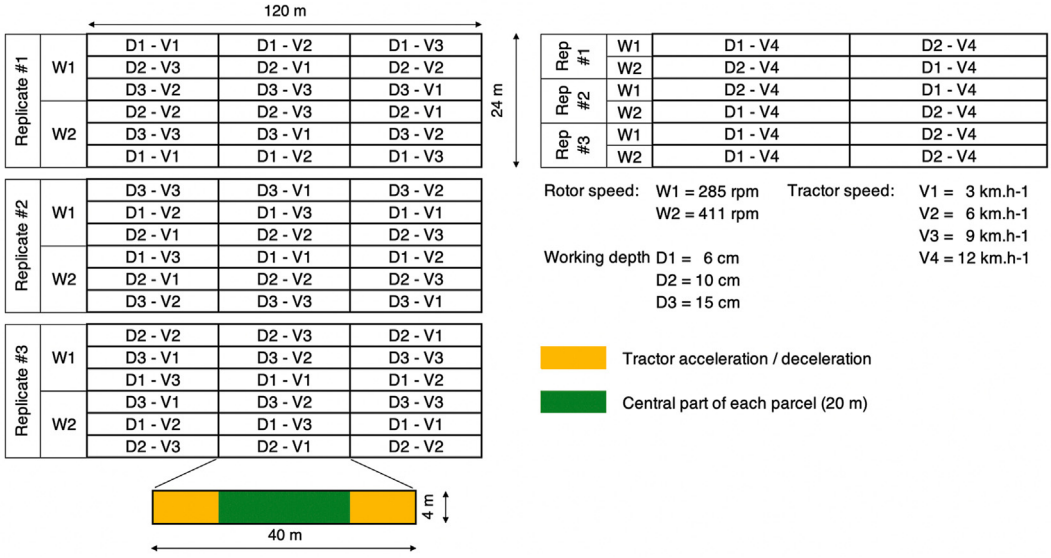

Fig. 1 – Scheme of the experimental design in a split-split-plot 2 × 3 × 3 factorial arrangement representing the different operating conditions.

in two separate files, first they were resampled according to the highest frequency. Then, the dataset was cleaned by excluding the values acquired when harrowing had not achieved the required tractor forward speed. In particular, the data acquired during tractor acceleration and deceleration was not included in the analysis.

The statistical analysis was performed by using the R software, version 3.6.0 (R Core Team, 2019). The data was analysed by using a linear mixed effect model (nlme package: Pinheiro, Bates, DebRoy, Sarkar, & R Core Team, 2019) where site, rotor speed, working depth and tractor speed were considered as fixed effects. All two- and three-way interactions were included in the model. Random components specified the three nested structures representing the three levels of blocking created in the split-split plot structures.

The data was visually checked for normality distribution and residual dispersions. When trends evidenced clear deviations from the assumptions, the data was log transformed and assumptions checked again. Treatment effects were separated by means of Bonferroni post hoc test procedures. The statistical results are reported at a 5% significance level.

3. Results and discussion

The average values of the measured tillage depths were close to the set values in all conditions, even if a different behaviour was observed due to the increase of soil compactness with depth. In particular, the achieved working depth was on average greater than the set values of 6 cm and 9 cm and lower than the nominal value of 15 cm (Table 3).

The PTO torque and draught data was collected from a total of 108 parcels (sites A and B) under different working conditions levels. The measured fluctuations of the PTO speed, set at the nominal value of 1000 rpm, during the experiments was in the range of ±20 rpm.

Table 3 – Measured working depths achieved during tillage with respect to the set values.

	Set working depth [cm]	Measured working depth [cm]	Average working depth [cm]
Site A	6.0	6.0–7.5	6.5
	10.0	9.0–11.0	10.3
	15.0	12.0–14.0	13.9
Site B	6.0	6.0–8.0	7.1
	10.0	9.0–11.5	10.7
	15.0	13.0–14.5	14.3

3.1. PTO torque

Based on 54 parcels of valid data for each site, the average PTO torque values were in the range of 90–620 Nm and 80–565 Nm, for sites A and B respectively. The PTO torque values were affected by the working parameters adopted and by the test site field.

3.1.1. Effects of working depth and tractor speed

The results showed how the working depth of the harrow rotors and the tractor speed significantly affected PTO torque values (Fig. 2). The average PTO torque varied from 116 Nm at a 6 cm working depth and 3 km h^{-1} tractor speed to 480 Nm at a 15 cm working depth and 9 km h^{-1} tractor speed. The average PTO torques were 215, 271 and 391 Nm for speeds of 3, 6 and 9 km h^{-1} respectively. No statistical differences in the PTO torque values were detected between working depths of 10 and 15 cm when the tractor was travelling at 3 km h^{-1}.

Similar results were found by other authors; for example, Usaborisut and Prasertkan (2018) reported that the PTO power, which is related to the PTO torque, of a power harrow increased from 12.7 to 17.4 kW when the tractor speed increased from

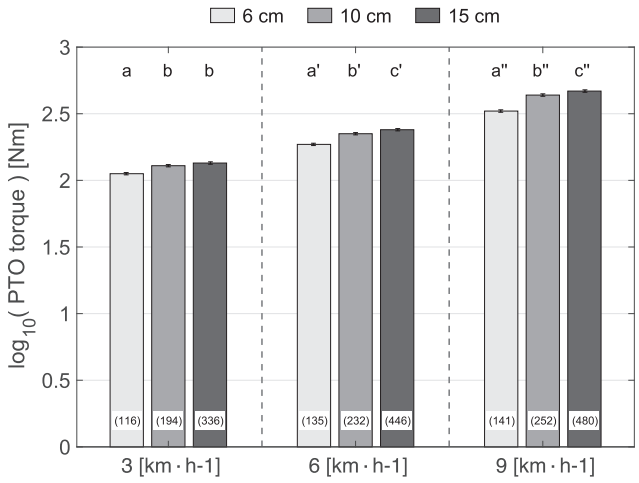

Fig. 2 – Average of the PTO torque values [Nm], expressed in log_{10}, for different harrow rotor working depths for each tractor speed. The average values at different depths were separated within each tractor speed by means of the Bonferroni post hoc test (p-value < 0.05). The error bars represent the standard error of the average values. The average of the untransformed data in [Nm] is in brackets.

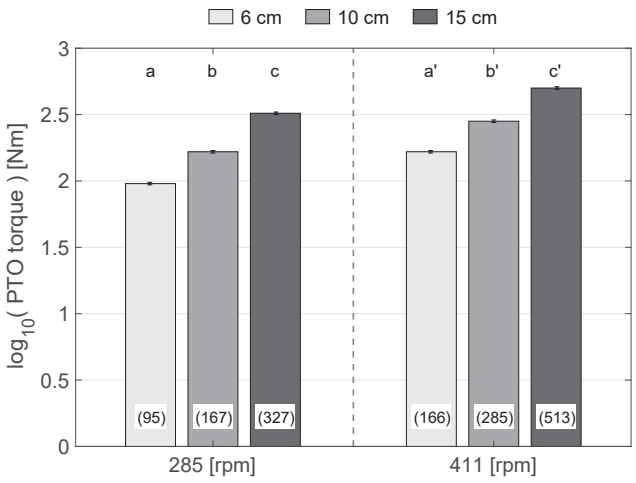

Fig. 3 – Average of the PTO torque values [Nm], expressed in log_{10}, for different harrow rotor working depths for each rotor speed. The average values at different depths were separated within each rotor speed by means of the Bonferroni post hoc test (p-value < 0.05). The error bars represent the standard error of the average values. The average of the untransformed data in [Nm] is in brackets.

1.79 to 3.33 km h^{-1}. Other researchers such as Upadhyaya, Williams, Kemble, and Collins (1984) and Weise (1993) have measured PTO power as a function of the tractor speed for two different machines, a ripper combined with a spider and a combined machine (wing tines and rotary tiller) respectively. They concluded that increasing the tractor speed resulted in a higher PTO power. Also, Shinners, Wilkes, and England (1993) tested a combined spring-cushioned tines and rotary tiller and the PTO power increased (34.0–53.4 kW) when the tractor speed increments (4.8–8.0 km h^{-1}).

3.1.2. *Effects of working depth and rotor speed*

The results in terms of average PTO torque as a function of the rotor working depth and rotational speed are reported in Fig. 3. The interaction of working depth and rotor speed was found to be statistically significant for PTO torque values. Indeed, the average PTO torque increased when the working depth as well as the rotor speed increase (Fig. 3). More in details, when the rotor speed increases from 285 to 411 rpm for each working depth, the average PTO torque increased by at least 55%. The average PTO torque was 196 Nm and 321 Nm in case of 285 and 411 rpm respectively.

Similar findings were obtained by Usaborisut and Prasertkan (2018), who detected an increase in the average PTO power (12.3–18.3 kW) when the harrow rotor speed increased from 299 to 526 rpm. Likewise, Kouchakzadeh and Haghighi (2011) found that when increasing the rotors speed, PTO torque increases remarkably.

3.1.3. *Effects of rotor speed and tractor speed*

The PTO torque values were found to be significantly affected by rotor and tractor speeds. Figure 4 shows the torque values as a function of the rotor speed for each tractor speed. The PTO torque increased when the rotor speed increases and it can also be noticed that the average PTO torque at a tractor speed of 9 km h^{-1} was more than 25% higher compared to a speed of 3 km h^{-1}.

The absolute speed of a rotor tine is obtained by combining two vectors: the tractor speed and the rotor tangent speed. Therefore, in a Cartesian coordinates system (with the *x* axis representing the tractor direction), the trajectory of each rotor tine can be represented by a prolate trochoid curve (Raparelli et al., 2020). The higher the tractor speed, the higher the relative speed of the rotor tine with respect to the soil, thus causing the viscous friction and the resistant torque to

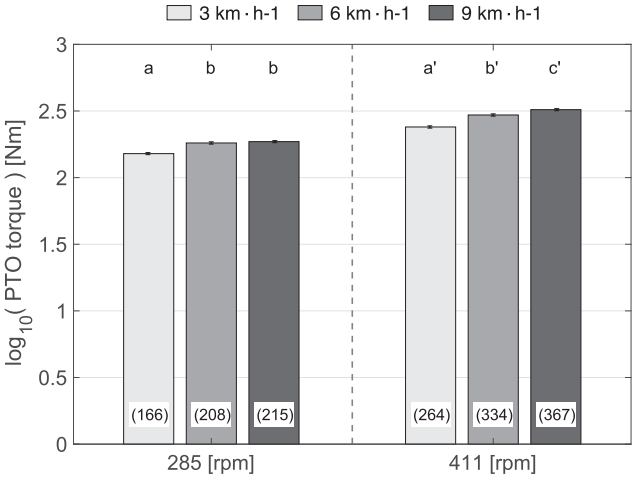

Fig. 4 – Average of the PTO torque values [Nm], expressed in log_{10}, for different rotor speeds for each tractor speed. The average values at different tractor speeds were separated within each rotor speed by means of the Bonferroni post hoc test (p-value < 0.05). The error bars represent the standard error of the average values. The average of the untransformed data in [Nm] is in brackets.

increase. This is a possible explanation for the increment in the PTO torque when increasing the tractor speed.

3.1.4. *Effects of working depth and test site field*

The PTO torque data collected in the field was found to be significantly affected by the working depth of the rotor tines and test site field at a 5% significance level. Figure 5 shows the torque values as a function of the harrow rotor working depth for sites A and B. The PTO torque values sharply increased when the rotor working depth increases. As can be seen, for both sites, the average PTO torque at a working depth of 15 cm was more than three times that at 6 cm. This can be justified by the higher volume of harrowed soil when increasing the working depth.

In Fig. 5, it can be noticed that the average PTO torque was 278 Nm and 240 Nm in sites A and B, respectively. Differences in the average values are due to soil properties, in particular soil in site A showed a higher cohesion than soil in site B (Table 2), although the two soils were quite similar in terms of texture. The different shear strength values were probably due to the different levels of moisture content of the two soils (greater in site B) as reported by Arvidsson et al. (2004), who found a cohesion decrease when the water content increases.

3.1.5. *PTO torque at the tractor speed of 12 km h^{-1}*

The PTO torque values at 12 km h^{-1} proved to be, on average, 227 Nm and 179 Nm, for sites A and B respectively. The overall average of the PTO torque at 12 km h^{-1} was 203 Nm, that is 31%, 10% and 3% higher than the overall average at 3, 6 and 9 km h^{-1} respectively (excluding the values at a working depth of 15 cm).

Table 4 – Average of the PTO torque [Nm] at the tractor speed of 12 km h^{-1}.

Rotor speed [rpm]		285		411	
Working depth [cm]		6	10	6	10
PTO torque [Nm]	Site A	108	205	201	392
	Site B	95	154	172	293

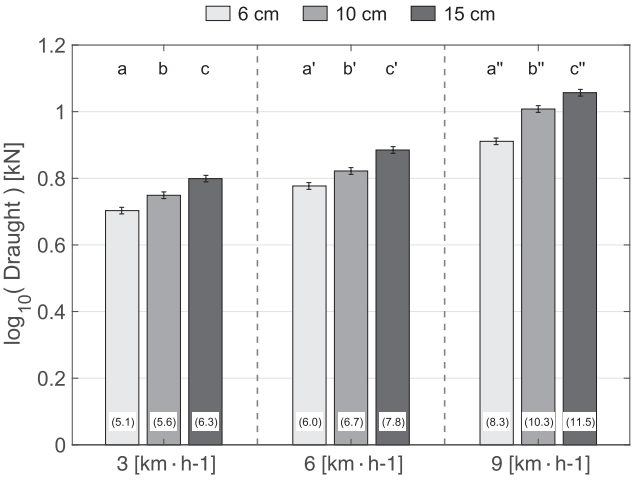

Fig. 6 – Average of the draught values [kN], expressed in $\log_{10}$, for different harrow rotor working depths for each tractor speed. The average values at different depths were separated within each tractor speed by means of the Bonferroni post hoc test (p-value < 0.05). The error bars represent the standard error of the average values. The average of the untransformed data in [kN] is in brackets.

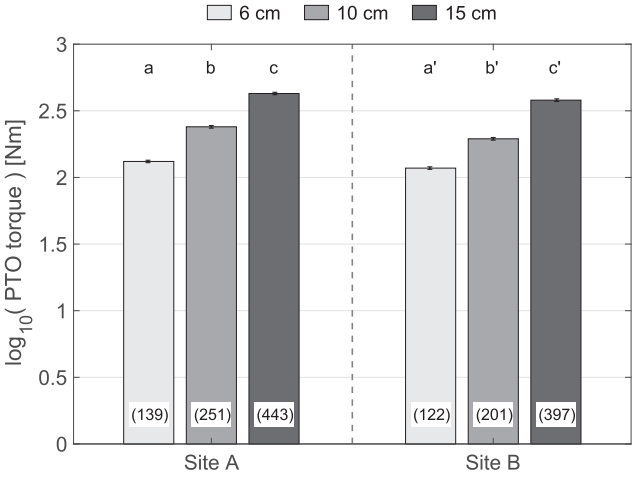

Fig. 5 – Average of the PTO torque values [Nm], expressed in $\log_{10}$, for different harrow rotor working depths for each test site field. The average values at different depths were separated within each site by means of the Bonferroni post hoc test (p-value < 0.05). The error bars represent the standard error of the average values. The average of the untransformed data in [Nm] is in brackets.

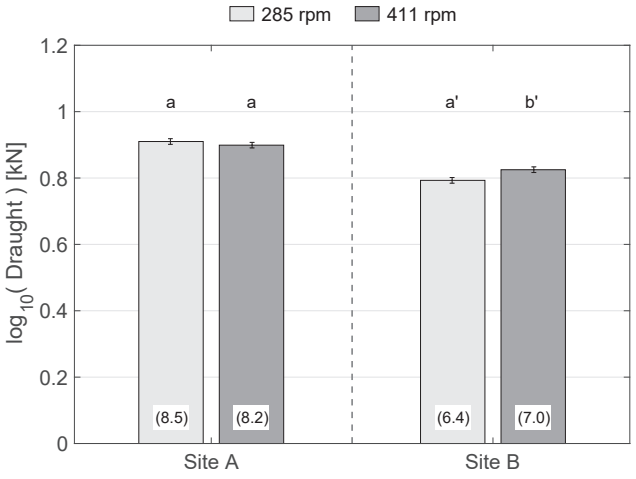

Fig. 7 – Average of the draught values [kN], expressed in $\log_{10}$, for different harrow rotor speeds for each test site field. The average values at different rotor speeds were separated within each site by means of the Bonferroni post hoc test (p-value < 0.05). The error bars represent the standard error of the average values. The average of the untransformed data in [kN] is in brackets.

The breakdown of the average PTO torque values was reported in Table 4. It can be noticed that the PTO torque increased when both rotor speed and working depth increase. The average PTO torque at 6 and 10 cm was 144 and 261 Nm respectively (Table 4). These latter two values are 24% and 35% higher than the ones measured at the same working depth and at the lowest tractor speed of 3 km h^{-1} (Fig. 2); the increment is only of 2% and 4% when the values are compared to 9 km h^{-1} (Fig. 2).

3.2. *Draught*

The results of the draught measured in 54 parcels for each site during harrowing, under different working conditions levels, are reported in Figs. 6 and 7. Significant effects for the rotor working depth, tractor speed, rotor speed and test site field on the draught were found.

3.2.1. *Effects of working depth and tractor speed*

The draught of the rotary harrow was found to increase when the tractor speed and the harrow working depth increment (Fig. 6). The average draught, taking into account the three nominal working depths (6, 10 and 15 cm), was 5.7, 6.8 and 10.0 kN at 3, 6 and 9 km h^{-1} respectively. Indeed, a high tractor speed results in a high shear rate and friction between the soil and the rotor tines, causing draught to increase.

The obtained results agree with previous published works. For example, Upadhyay and Raheman (2018) tested a powered disc harrow and obtained increments of 43.6%, 31.8% and 36.6%, at 9, 12 and 14 cm working depths respectively, when the tractor speed was increased from 3.7 km h^{-1} to 6.6 km h^{-1}. Usaborisut and Prasertkan (2018) reported how the average draught of the tested rotary harrow increased from 31.3 to 35.1 kN when the tractor speed increases from 1.79 to 3.33 km h^{-1}. Similar results were found by Ranjbarian, Mohammad, and Jannatkhah (2017), who measured the draught for three different implements (mouldboard plough, disc plough and chisel plough) at four tractor speeds. They showed how the draught increased when the tractor speed increases. Also, Sahu and Raheman (2006) obtained a draught increment when the speed of the tested cultivator with a disk gang increased. It is conceivable that the higher the tractor speed, the higher the shear rate between soil and metal will be, thus leading to higher draught.

Upadhyay and Raheman (2018), Sahu and Raheman (2006) and Grisso et al. (1996) have found that the draught was significantly affected (p-value < 0.05) by the working depth. This is mostly due to a larger volume of tilled soil and the wider interface area between the rotor tines and the soil.

Table 5 – Average draught [kN] at the tractor speed of 12 km h^{-1}.

Rotor speed [rpm]		285		411	
Working depth [cm]		6	10	6	10
Draught [kN]	Site A	7.5	9.5	7.1	10.3
	Site B	5.8	7.3	6.6	7.6

3.2.2. *Effects of rotor speed and test site field*

The draught data collected during field operations was found to be significantly affected by test site field and rotor speed as shown in Fig. 7. Since soil in site A is firmer than soil in site B (Table 2), the average draught was found to be 25% higher than the average draught in site B.

In the case of site A, the average draught decreased from 8.5 to 8.2 kN when the rotor speed was increased from 285 to 411 rpm. Similar results were obtained by Usaborisut and Prasertkan (2018). However, the average draught for site A at a different rotor speed was not found to be statistically different. In the case of site B, the average draught values increased slightly when the rotor speed increases.

3.2.3. *Draught at the tractor speed of 12 km h^{-1}*

The draught values at the tractor speed of 12 km h^{-1} were 8.6 kN and 6.8 kN (Table 5), for sites A and B respectively

Table 6 – Power, energy and fuel consumption values at different working conditions of the tractor - power harrow system for site A (rotor speed fixed at 285 rpm).

Working depth [cm]		6			10			15		
Tractor speed [km h^{-1}]		3	6	9	3	6	9	3	6	9
Power [kW]	PTO	9.6	11.1	11.1	16.5	20.5	21.4	29.1	38.7	42.0
	Draught	5.1	10.7	17.6	5.7	13.2	21.4	8.4	20.6	33.7
	Total	14.7	21.8	28.7	22.2	33.7	42.8	37.5	59.3	75.7
Power [kW m^{-3}]	PTO	2.7	3.1	3.1	2.7	3.4	3.6	3.2	4.3	4.7
	Draught	1.4	3.0	4.9	1.0	2.2	3.6	0.9	2.3	3.7
	Total	4.1	6.1	8.0	3.7	5.6	7.2	4.1	6.6	8.4
Energy [kWh]	PTO	0.062	0.036	0.024	0.107	0.066	0.046	0.188	0.125	0.090
	Draught	0.033	0.034	0.038	0.037	0.043	0.046	0.054	0.067	0.073
	Total	0.095	0.070	0.062	0.144	0.109	0.092	0.242	0.192	0.163
Energy [kWh m^{-3}]	PTO	0.017	0.010	0.007	0.018	0.011	0.008	0.021	0.014	0.010
	Draught	0.009	0.010	0.011	0.006	0.007	0.008	0.006	0.007	0.008
	Total	0.026	0.020	0.018	0.024	0.018	0.016	0.027	0.021	0.018
Energy [kWh ha^{-1}]	PTO	10.4	6.0	4.0	17.8	11.0	7.7	31.3	20.8	15.1
	Draught	5.5	5.7	6.3	6.2	7.1	7.7	9.0	11.1	12.1
	Total	15.9	11.7	10.3	24.0	18.1	15.4	40.3	31.9	27.2
Fuel	[l h^{-1}]	14.0	19.8	23.1	16.7	21.8	25.5	20.2	26.8	33.3
	[l ha^{-1}]	15.1	10.7	8.2	18.0	11.7	9.1	21.7	14.4	12.0

(including the two rotor speeds and working depths). The overall average of the draught at 12 km h^{-1} was 7.7 kN, which is 43%, 20% and −17% higher or lower than the overall average at 3, 6 and 9 km h^{-1} respectively (excluding the values at a working depth of 15 cm). The average at 12 km h^{-1} turned out to be lower than the one at 9 km h^{-1} as the working depth within the plots was limited at 9 cm.

The breakdown of the average draught values at 12 km h^{-1} was reported in Table 5. It can be noticed how the draught decreases when the rotor speed increases. The average draught at 6 and 10 cm was 6.8 and 8.7 kN respectively. The average draught at 6 and 10 cm, when the tractor travelled at 3 km h^{-1}, was 33% and 57% lower than the draught measured at the tractor speed of 12 km h^{-1} and at the same working depth, while the draught values at 9 km h^{-1} were 22% and 18% higher than those at 12 km h^{-1} (working depths of 6 and 10 cm).

3.3. Power and energy consumption for tilling operations

The PTO and draught powers were evaluated according to the monitored PTO speed and tractor speed respectively. The power and energy data was not considered in the statistical analysis as a linear combination of PTO torque and draught values (§ 3.1 and 3.2). The analysed power and energy data is shown in Tables 6 and 7 for site A and Tables 8 and 9 for site B.

As expected, the total power, which is the sum of the PTO and draught contributions, was found to increase when the working depth, tractor speed and rotor speed increase (Tables 6–9). The parameters that mostly affected the PTO power were the speed and the working depth of the rotors. Indeed, the PTO power increased by more than 50% when the rotor speed was modified from 285 to 411 rpm (at fixed working

Table 7 – Power, energy and fuel consumption values at different working conditions of the tractor - power harrow system for site A (rotor speed fixed at 411 rpm).

Working depth [cm]		6			10			15		
Tractor speed [km h^{-1}]		3	6	9	3	6	9	3	6	9
Power [kW]	PTO	15.5	19.3	20.5	26.5	33.7	38.9	44.3	61.1	65.5
	Draught	4.8	10.7	17.4	5.7	12.5	24.8	8.3	18.8	24.7
	Total	20.3	30.0	37.9	32.2	46.2	63.7	52.6	79.9	90.2
Power [kW m^{-3}]	PTO	4.3	5.4	5.7	4.4	5.6	6.5	4.9	6.8	7.3
	Draught	1.3	3.0	4.8	1.0	2.1	4.1	0.9	2.1	2.7
	Total	5.6	8.4	10.5	5.4	7.7	10.6	5.8	8.9	10.0
Energy [kWh]	PTO	0.100	0.062	0.044	0.171	0.109	0.083	0.286	0.197	0.167
	Draught	0.031	0.035	0.037	0.037	0.040	0.053	0.054	0.061	0.063
	Total	0.131	0.097	0.081	0.208	0.149	0.136	0.340	0.258	0.230
Energy [kWh m^{-3}]	PTO	0.028	0.017	0.012	0.028	0.018	0.014	0.032	0.022	0.019
	Draught	0.009	0.010	0.010	0.006	0.007	0.009	0.006	0.007	0.007
	Total	0.037	0.027	0.022	0.034	0.025	0.023	0.038	0.029	0.026
Energy [kWh ha^{-1}]	PTO	16.6	10.4	7.4	28.5	18.1	13.9	47.6	32.8	27.9
	Draught	5.1	5.8	6.3	6.1	6.7	8.9	8.9	10.1	10.5
	Total	21.7	16.2	13.7	34.6	24.8	22.8	56.5	42.9	38.4
Fuel	[l h^{-1}]	15.6	21.2	24.4	19.2	24.4	29.7	23.1	31.9	35.4
	[l ha^{-1}]	16.8	11.4	8.4	20.7	13.1	10.6	24.8	17.1	15.1

Table 8 – Power, energy and fuel consumption values at different working conditions of the tractor - power harrow system for site B (rotor speed fixed at 285 rpm).

Working depth [cm]		6			10			15		
Tractor speed [km h^{-1}]		3	6	9	3	6	9	3	6	9
Power [kW]	PTO	8.7	9.8	9.8	14.7	16.2	15.8	26.5	35.2	35.7
	Draught	3.9	8.7	14.4	4.5	10.6	16.3	5.7	14.9	26.5
	Total	12.6	18.5	24.2	19.2	26.8	32.1	32.2	50.1	62.2
Power [kW m^{-3}]	PTO	2.4	2.7	2.7	2.5	2.7	2.6	3.0	3.9	4.0
	Draught	1.1	2.4	4.0	0.7	1.8	2.7	0.6	1.7	2.9
	Total	3.5	5.1	6.7	3.2	4.5	5.3	3.6	5.6	6.9
Energy [kWh]	PTO	0.056	0.032	0.021	0.093	0.052	0.034	0.171	0.114	0.077
	Draught	0.025	0.028	0.031	0.028	0.034	0.035	0.037	0.048	0.057
	Total	0.081	0.060	0.052	0.121	0.086	0.069	0.208	0.162	0.134
Energy [kWh m^{-3}]	PTO	0.016	0.009	0.006	0.015	0.009	0.006	0.019	0.013	0.009
	Draught	0.007	0.008	0.009	0.005	0.006	0.006	0.004	0.005	0.006
	Total	0.023	0.017	0.015	0.020	0.015	0.012	0.023	0.018	0.015
Energy [kWh ha^{-1}]	PTO	9.3	5.3	3.5	15.5	8.7	5.7	28.5	18.9	12.8
	Draught	4.2	4.7	5.2	4.7	5.7	5.8	6.1	8.0	9.5
	Total	13.5	10.0	8.7	20.2	14.4	11.5	34.6	26.9	22.3
Fuel	[l h^{-1}]	12.8	18.5	22.4	15.9	19.5	22.8	19.1	24.2	30.1
	[l ha^{-1}]	13.7	10.0	8.0	16.8	10.5	8.2	20.5	13.0	10.8

depth and tractor speed). Moreover, the PTO power sharply increased, more than twice, when the working depth increases (at fixed rotor speed and tractor speed). The highest total PTO power was obtained in the case of site A, which was 90.2 kW (Table 7). Also, Fig. 8 shows the total PTO power values at a tractor speed of 12 km h^{-1}.

Tables 6–9 also report the power per unit of volume of the tilled soil [kW m^{-3}]. The specific power increases when increasing the three working parameters; however, it can be noticed that when comparing the specific powers at different working depths, at fixed tractor speed and rotor speed, the values do not change dramatically but are quite similar (in the range of ±10%). This has an impact not only for farmers but also for tractors and power harrows manufacturers as they can use such data in the design phase (the statement is valid for the tested type of soil).

Table 9 – Power, energy and fuel consumption values at different working conditions of the tractor - power harrow system for site B (rotor speed fixed at 411 rpm).

Working depth [cm]		6			10			15		
Tractor speed [km h^{-1}]		3	6	9	3	6	9	3	6	9
Power [kW]	PTO	15.0	16.5	17.6	23.8	27.0	29.8	41.8	53.1	59.1
	Draught	3.9	8.8	16.2	5.0	10.0	18.4	6.2	16.8	27.4
	Total	18.9	25.3	33.8	28.8	37.0	48.2	48.0	69.9	86.5
Power [kW m^{-3}]	PTO	4.2	4.6	4.9	4.0	4.5	5.0	4.6	5.9	6.6
	Draught	1.1	2.4	4.5	0.8	1.7	3.1	0.7	1.9	3.0
	Total	5.3	7.0	9.4	4.8	6.2	8.1	5.3	7.8	9.6
Energy [kWh]	PTO	0.097	0.053	0.038	0.153	0.087	0.063	0.269	0.171	0.136
	Draught	0.025	0.028	0.035	0.032	0.032	0.039	0.040	0.054	0.063
	Total	0.122	0.081	0.073	0.185	0.119	0.102	0.309	0.225	0.199
Energy [kWh m^{-3}]	PTO	0.027	0.015	0.011	0.026	0.015	0.011	0.030	0.019	0.015
	Draught	0.007	0.008	0.010	0.005	0.005	0.007	0.004	0.006	0.007
	Total	0.034	0.023	0.021	0.031	0.020	0.018	0.034	0.025	0.022
Energy [kWh ha^{-1}]	PTO	16.1	8.9	6.3	25.6	14.5	10.5	44.9	28.6	22.6
	Draught	4.2	4.7	5.8	5.4	5.4	6.5	6.6	9.1	10.4
	Total	20.3	13.6	12.1	31.0	19.9	17.0	51.5	37.7	33.0
Fuel	[l h^{-1}]	16.1	19.5	22.6	18.4	22.3	25.6	22.1	28.2	34.5
	[l ha^{-1}]	17.3	10.5	8.1	19.8	12.0	9.0	23.8	15.1	13.2

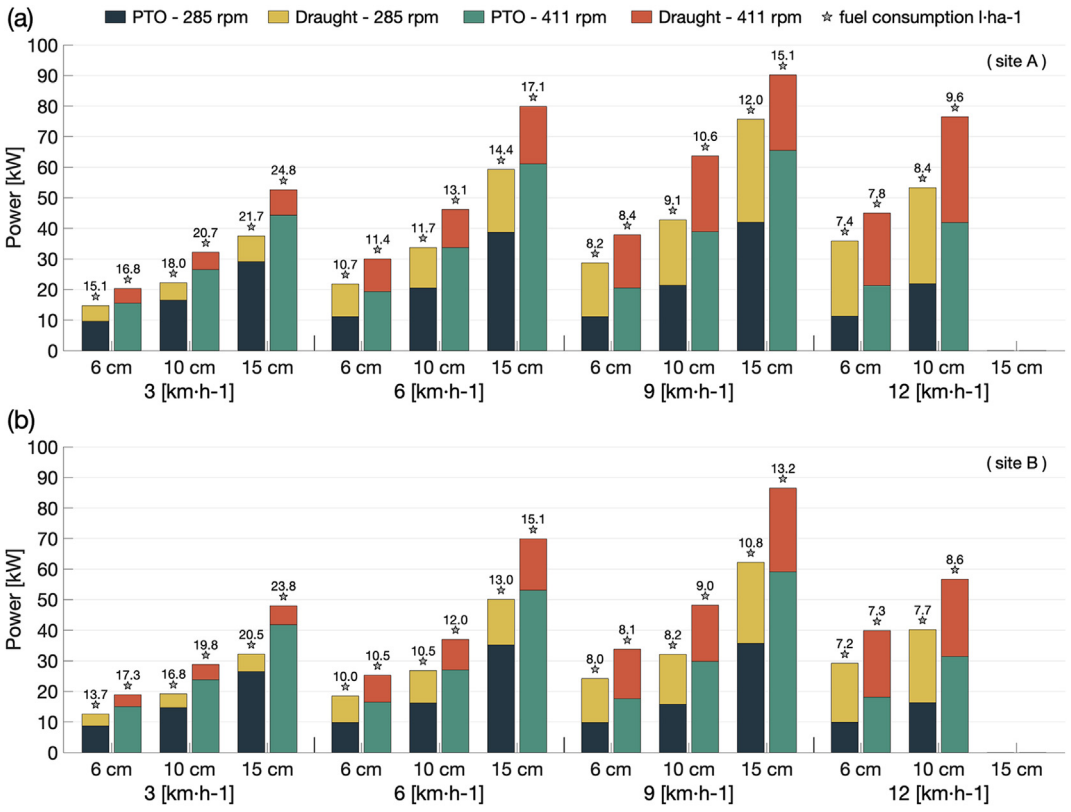

Fig. 8 – Average power [kW] required by the power harrow at different tractor speeds, rotor working depths and rotor speeds for site A (a) and site B (b). Fuel consumption [l ha^{-1}] of the tractor is indicated by the numbers above the grey stars.

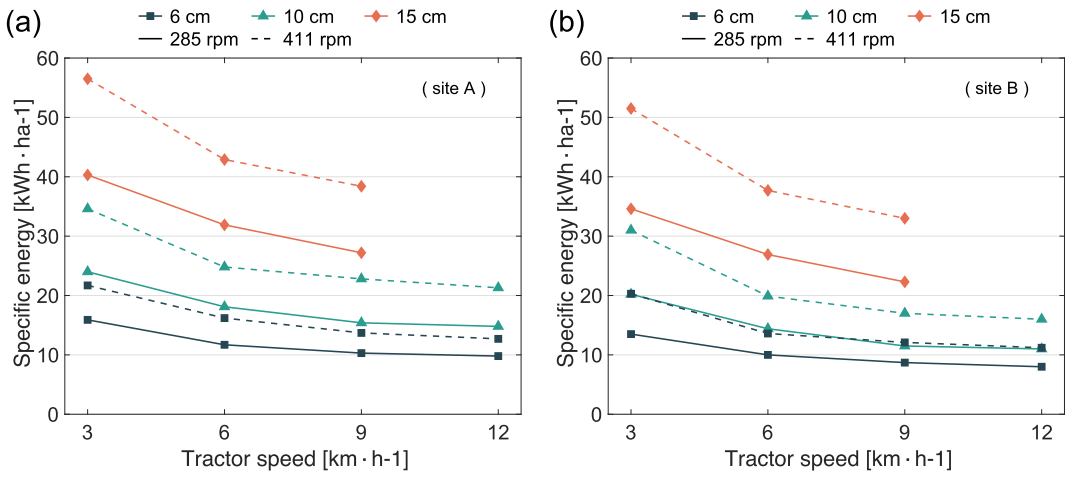

Fig. 9 – Average of the total specific energy [kWh ha^{-1}] required by the power harrow at different tractor speeds, rotor working depths and rotor speeds for site A (a) and site B (b).

The PTO and draught energy values [kWh] shown in Tables 6–9 were obtained by considering the time taken to till 20 m of each parcel (§ 2.4). The energy values per unit of volume and surface of tilled soil are also reported in the same Tables. These specific PTO energy values decrease when the tractor speed increases, while the draught energy values increase at higher tractor speeds (at fixed working depth and rotor speed). However, in this configuration, the draught energy increment is lower than the PTO energy increment, thus causing the total energy to decrease when the tractor speed increases. Also, the specific energy values were found to decrease when the tractor speed was increased from 3 to 12 km h^{-1} (Fig. 9).

Tables 6–9 also report the fuel consumption in l h^{-1} and l ha^{-1} for each combination of working conditions. It can be noticed that fuel consumption in l ha^{-1} decreases when the tractor speed increases; this is due to the time reduction in harrowing. However, the choice of the working parameters cannot only be based on fuel consumption as tillage operations strictly depend on the type of crop to be seeded, and consequently on the required soil cloddiness. Figure 10 shows the percentage by weight of soil aggregates having an equivalent diameter lower than 10 mm at different tractor speeds for sites A and B respectively. The data in Fig. 10 refers to a rotor speed of 285 rpm, which is more critical with regards to soil fragmentation when compared to a rotor speed of 411 rpm. It can be noticed that the percentage of soil aggregates mass in site A as well as in site B, with a size lower than 10 mm, was higher when the tractor was travelling at the lowest tractor speed (3 km h^{-1}). In sites A and B, the percentage of soil aggregates lower than 10 mm, at tractor speeds between 6 and 12 km h^{-1}, was found to be quite similar (Fig. 10). On average, the percentage of soil aggregates lower than 10 mm turned out to be higher in site B than in site A.

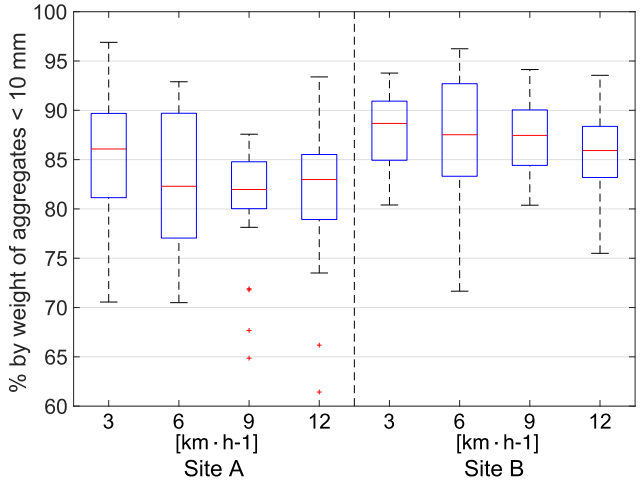

Fig. 10 – Percentage by weight of soil aggregates having an equivalent diameter lower than 10 mm at different tractor speeds for sites A and B respectively. The data refers to rotor speed 285 rpm.

4. Conclusions

This paper presents the results of an extensive in-field experimental campaign in which the behaviour of several indicators (PTO torque, draught and fuel consumption) of a tractor - power harrow system was monitored under different working conditions (tractor speed, rotor speed, working depth of the rotor tines) in two different test site fields. The data was acquired from more than 100 plots and statistically analysed by using the R software (nlme package and Bonferroni post hoc tests). The results showed that PTO torque and draught varied significantly according to the different working conditions.

The in-field tests were conducted up to a tractor speed of 12 km h^{-1}, which is, nowadays, rather high for this kind of tested implement, but it might become a target speed in the near future, especially when the harrow is coupled to a seeder. The presented results also show that both the total (PTO + draught) specific energy in kWh ha^{-1} and the fuel consumption in l ha^{-1} decrease when increasing the tractor speed for site A as well as for site B (Tables 6–9 and Figs. 8 and

9). Moreover, the quality of the soil in terms of soil fragmentation was found to be adequate for sowing (size of soil aggregates lower than 10 mm) even at a tractor speed higher than 3 km h^{-1} (Fig. 10). These results are thus crucial to farmers, who are then able to find appropriate working condition settings to limit the running costs of the tillage. For example, depending on the specific crop, the first tillage run may be performed at 3 km h^{-1} while the second at 6 or 9 km h^{-1}. In many cases, the higher speed of the second tillage may be set to match to the recommended working speed of the seeder, possibly coupled to the harrow.

The mechanical loads concerning PTO torque and draught, measured in different operative parameters scenarios, may also be useful to agricultural machinery manufacturers, who may properly design mechanical structures and ball bearings for power harrows.

Dedication

Dario Sacco was born in Italy, near Turin, on 15 May 1970. He received his M.Sc. in Agricultural Science from the University of Turin, and his Ph.D in Agronomy from the University of Florence in 2000. Assistant Professor from 2008, he was promoted to Associate Professor in Agronomy and Crop Science in 2014 at the Department of Agricultural, Forest and Food Sciences (DiSAFA, University of Turin). In Italy, he was one of the most important experts in Agricultural applications of Statistics. His research interests included: indicator tools assessing cropping system sustainability, rice management and GHG emission in paddy fields, soil OM and N turnover, remote sensing, and spatial data applications to agriculture. He passed away on 8 August 2020 while being on holiday with his beloved family. The authors would like to dedicate this paper to his memory and together with all the people of the Department (DiSAFA, University of Turin) would like to express their sorrow for his premature death.

Declaration of Competing Interest

The authors declare that they have no known competing financial interests or personal relationships that could have appeared to influence the work reported in this paper.

Acknowledgments

This research was funded by the Italian Ministry of University and Research (MIUR), PRIN 2015 "Ottimizzazione di macchine operatrici attraverso l'analisi del profilo di missione per un'agricoltura più efficiente" (Prot. 2015KTY5NW).

The authors would like to acknowledge Frandent Group Srl for making the power harrow and the test fields available, and the partners of the GreenTillage project for their collaboration. Also, the authors would like to express their special thanks to the farm Fratelli Tamagnone s.a.s., Poirino (TO) - Italy, for hosting the experiments.

REFERENCES

Acharya, B. S., Dodla, S., Gaston, L. A., Darapuneni, M., Wang, J. J., Sepat, S., et al. (2019). Winter cover crops effect on soil moisture and soybean growth and yield under different tillage systems. *Soil and Tillage Research, 195*, 104430. https://doi.org/10.1016/j.still.2019.104430

Adam, K. M., & Erbach, D. C. (1992). Secondary tillage tool effect on soil aggregation. *Transactions of the American Society of Agricultural Engineers, 35*, 1771–1776. https://doi.org/10.13031/2013.28796

Aday, S. H. (2015). *Theory of agricultural machines*. Basrah, Iraq: Algadeer Co. for Printing and Publishing.

Ahmadi, I. (2017). A torque calculator for rotary tiller using the laws of classical mechanics. *Soil and Tillage Research, 165*, 137–143. https://doi.org/10.1016/j.still.2016.08.009

Arvidsson, J., Keller, T., & Gustafsson, K. (2004). Specific draught for mouldboard plough, chisel plough and disc harrow at different water contents. *Soil and Tillage Research, 79*, 221–231. https://doi.org/10.1016/j.still.2004.07.010

ASABE Standards. (2006). Agricultural machinery management. *EP 496, 3*, 385–390.

ASABE Standards. (2018). *Procedures for using and reporting data obtained with the soil cone penetrometer* (Vol. 542). EP.

ASTM International. (2019). *C136/C136M – 14. Standard test method for sieve analysis of fine and coarse aggregates*.

Berntsen, R., & Berre, B. (2002). Soil fragmentation and the efficiency of tillage implements. *Soil and Tillage Research, 64*, 137–147. https://doi.org/10.1016/S0167-1987(01)00251-3

Braunack, M. V. (1995). Effect of aggregate size and soil water content on emergence of soybean (*Glycine max*, L. Merr.) and maize (*Zea mays*, L.). *Soil and Tillage Research, 33*, 149–161. https://doi.org/10.1016/0167-1987(94)00444-J

Braunack, M. V., & Dexter, A. R. (1989). Soil aggregation in the seedbed: A review. I. Properties of aggregates and beds of aggregates. *Soil and Tillage Research, 14*, 259–279. https://doi.org/10.1016/0167-1987(89)90013-5

Calcante, A., & Oberti, R. (2019). A technical-economic comparison between conventional tillage and conservative techniques in paddy-rice production practice in Northern Italy. *Agronomy, 9*, 886. https://doi.org/10.3390/agronomy9120886

Chan, C. W., Wood, R. K., & Holmes, R. G. (1993). Powered harrow operating parameters: Effects on soil physical properties. *Transactions of the American Society of Agricultural Engineers, 36*, 1279–1285. https://doi.org/10.13031/2013.28460

Čiplienė, A., Gurevičius, P., Janulevičius, A., & Damanauskas, V. (2019). Experimental validation of tyre inflation pressure model to reduce fuel consumption during soil tillage. *Biosystems Engineering, 186*, 45–59. https://doi.org/10.1016/j.biosystemseng.2019.06.023

Damanauskas, V., Velykis, A., & Satkus, A. (2019). Efficiency of disc harrow adjustment for stubble tillage quality and fuel consumption. *Soil and Tillage Research, 194*, 104311. https://doi.org/10.1016/j.still.2019.104311

Destain, M. F., & Houmy, K. (1990). Effects of design and kinematic parameters of rotary cultivators on soil structure. *Soil and Tillage Research, 17*, 291–301. https://doi.org/10.1016/0167-1987(90)90042-C

Dürr, C., & Aubertot, J. N. (2000). Emergence of seedlings of sugar beet (*Beta vulgaris* L.) as affected by the size, roughness and position of aggregates in the seedbed. *Plant and Soil, 219*, 211–220.

Garcia-Franco, N., Albaladejo, J., Almagro, M., & Martínez-Mena, M. (2015). Beneficial effects of reduced tillage and green manure on soil aggregation and stabilization of organic carbon in a Mediterranean agroecosystem. *Soil and Tillage Research, 153*, 66–75. https://doi.org/10.1016/j.still.2015.05.010

Gee, G. W., & Bauder, J. W. (1986). Particle-size analysis. In *Methods of soil analysis: Part 1* (2nd ed., Vol. 9, pp. 383–411). A. Klute. *Agronomy Monograph*.

Grisso, R. D., Vaughan, D. H., & Roberson, G. T. (2008). Fuel prediction for specific tractor models. *Applied Engineering in Agriculture, 24*, 423–428. https://doi.org/10.13031/2013.25139

Grisso, R. D., Yasin, M., & Kocher, M. F. (1996). Tillage implement forces operating in silty clay loam. *Transactions of the ASAE, 39*, 1977–1982. https://doi.org/10.13031/2013.27699

Håkansson, I., Myrbeck, Å., & Etana, A. (2002). A review of research on seedbed preparation for small grains in Sweden. *Soil and Tillage Research, 64*, 23–40. https://doi.org/10.1016/S0167-1987(01)00255-0

Hendrick, J. G. (1969). Depth, direction of rotation and peripheral to forward velocity ratio as design parameters of rotary tillers. *Asae, 69*, 661.

Hendrick, J. G., & Gill, W. R. (1978). Rotary tiller design parameters, V:Kinematics. *Transactions of the American Society of Agricultural Engineers, 21*, 658–660. https://doi.org/10.13031/2013.35362

Kayad, A., Rainato, R., Picco, L., Sartori, L., & Marinello, F. (2019). Assessing topsoil movement in rotary harrowing process by RFID (Radio-Frequency Identification) technique. *Agriculture, 9*, 184. https://doi.org/10.3390/agriculture9080184

Kheiralla, A. F., Yahya, A., Zohadie, M., & Ishak, W. (2004). Modelling of power and energy requirements for tillage implements operating in Serdang sandy clay loam, Malaysia. *Soil and Tillage Research, 78*, 21–34. https://doi.org/10.1016/j.still.2003.12.011

Kinzel, G. L., Holmes, R., & Huber, S. (1981). Computer graphics analysis of rotary tillers. *Transactions of the American Society of Agricultural Engineers, 24*, 1392–1395. https://doi.org/10.13031/2013.34458

Kogut, Z., Sergiel, L., & Żurek, G. (2016). The effect of the disc setup angles and working depth on disc harrow working resistance. *Biosystems Engineering, 151*, 328–337. https://doi.org/10.1016/j.biosystemseng.2016.10.004

Kouchakzadeh, A., & Haghighi, K. (2011). The effect of rototiller equipped with serrated blades on some soil properties. *International Research Journal of Applied and Basic Sciences, 2*, 209–215.

Krause, R., Lorenz, F., & Hoogmoed, W. B. (1984). *Soil tillage in the tropics and subtropics* (p. 320). Eschborn: GTZ. ISBN: 9783880852006.

Kursat Celik, H., Caglayan, N., Topakci, M., Rennie, A. E. W., & Akinci, I. (2020). Strength-based design analysis of a Para-Plow tillage tool. *Computers and Electronics in Agriculture, 169*, 105168. https://doi.org/10.1016/j.compag.2019.105168

Köppen, W. (1936). Das geographische system der climate. In *Handbuch der klimatologie. I, Teil, C.*. Berlin: Gebrüder Borntraeger.

Matin, Md. A., Fielke, J. M., & Desbiolles, J. M. A. (2014). Furrow parameters in rotary strip-tillage: Effect of blade geometry and rotary speed. *Biosystems Engineering, 118*, 7–15. https://doi.org/10.1016/j.biosystemseng.2013.10.015

Mattetti, M., Varani, M., Molari, G., & Morelli, F. (2017). Influence of the speed on soil-pressure over a plough. *Biosystems Engineering, 156*, 136–147. https://doi.org/10.1016/j.biosystemseng.2017.01.009

Nafi, E., Webber, H., Danso, I., Naab, J. B., Frei, M., & Gaiser, T. (2020). Interactive effects of conservation tillage, residue management, and nitrogen fertilizer application on soil properties under maize-cotton rotation system on highly weathered soils of West Africa. *Soil and Tillage Research, 196*, 104473. https://doi.org/10.1016/j.still.2019.104473

Navalade, P. P., Salokhe, V. M., Niyamapa, T., & Soni, P. (2010). Performance of free rolling and powered tillage discs. *Soil and Tillage Research, 109*, 87–93. https://doi.org/10.1016/j.still.2010.05.004

OECD. (2010). *Report n° 2/2 541. OECD Standard Code 2 for the official testing of agricultural and forestry tractor performance*. Paris, France: Organization for Economic Co-operation and Development.

Perdok, U. D., & Kouwenhoven, J. K. (1994). Soil-tool interactions and field performance of implements. *Soil and Tillage Research, 30*, 283–326. https://doi.org/10.1016/0167-1987(94)90008-6

Perdok, U. D., & Van de Werken, G. (1983). Power and labour requirements in soil tillage - a theoretical approach. *Soil and Tillage Research, 3*, 3–25. https://doi.org/10.1016/0167-1987(83)90013-2

Pinheiro, J., Bates, D., DebRoy, S., Sarkar, D., & R Core Team. (2019). *_nlme: Linear and nonlinear mixed effects models_. R package version 3.1-143*. https://CRAN.R-project.org/package=nlme.

Pitla, S. K., Luck, J. D., Werner, J., Lin, N., & Shearer, S. A. (2016). In-field fuel use and load states of agricultural field machinery. *Computers and Electronics in Agriculture, 121*, 290–300. https://doi.org/10.1016/j.compag.2015.12.023

R Core Team. (2019). *R: A language and environment for statistical computing*. Vienna, Austria: R Foundation for Statistical Computing. URL https://www.R-project.org/.

Ranjbarian, S., Mohammad, A., & Jannatkhah, J. (2017). Performance of tractor and tillage implements in clay soil. *Journal of Saudi Society of Agricultural Sciences, 16*, 154–162. https://doi.org/10.1016/j.jssas.2015.05.003

Raparelli, T., Pepe, G., Ivanov, A., & Eula, G. (2020). Kinematic analysis of rotary harrows. *Journal of Agricultural Engineering, 51*, 9–14. https://doi.org/10.4081/jae.2019.976

SAE. (2013). *Standard J1939: Serial control and communications heavy duty vehicle Network – top level document*. http://standards.sae.org/j1939_201308/.

Sahu, R. K., & Raheman, H. (2006). An approach for draft prediction of combination tillage implements in sandy loam soil. *Soil and Tillage Research, 90*, 145–155. https://doi.org/10.1016/j.still.2005.08.015

Schjønning, P., & Rasmussen, K. J. (2000). Soil strength and soil pore characteristics for direct drilled and ploughed soils. *Soil and Tillage Research, 57*, 69–82. https://doi.org/10.1016/S0167-1987(00)00149-5

Serrano, J. M., Peça, J. O., Marques da Silva, J., Pinheiro, A., & Carvalho, M. (2007). Tractor energy requirements in disc harrow systems. *Biosystems Engineering, 98*, 286–296. https://doi.org/10.1016/j.biosystemseng.2007.08.002

Shinners, K. J., Wilkes, J. M., & England, T. D. (1993). Performance characteristics of a tillage machine with active–passive components. *Journal of Agricultural Engineering Research, 55*, 277–297. https://doi.org/10.1006/jaer.1993.1050

Sijtsma, C. H., Campbell, A. J., McLaughlin, N. B., & Carter, M. R. (1998). Comparative tillage costs for crop rotations utilizing minimum tillage on a farm scale. *Soil and Tillage Research, 49*, 223–231. https://doi.org/10.1016/S0167-1987(98)00175-5

Tagar, A. A., Adamowski, J., Memon, M. S., Do, M. C., Mashori, A. S., Soomro, A. S., et al. (2020). Soil fragmentation

and aggregate stability as affected by conventional tillage implements and relations with fractal dimensions. *Soil and Tillage Research, 197*, 104494. https://doi.org/10.1016/j.still.2019.104494

United States Department of Agriculture (USDA), & Natural Resources Conservation Service (NRCS). (2012). In *Chapter 3, engineering classification of earth materials, National engineering handbook, Part 631*. Washington, DC: Dams.

Upadhyaya, S. K., Williams, T. H., Kemble, L. J., & Collins, N. E. (1984). Energy requirements for chiseling in coastal plain soils. *Transactions of the American Society of Agricultural Engineers, 27*, 1643–1649. https://doi.org/10.13031/2013.33019

Upadhyay, G., & Raheman, H. (2018). Performance of combined offset disc harrow (front active and rear passive set configuration) in soil bin. *Journal of Terramechanics, 78*, 27–37. https://doi.org/10.1016/j.jterra.2018.04.002

Upadhyay, G., & Raheman, H. (2019). Comparative analysis of tillage in sandy clay loam soil by free rolling and powered disc harrow. *Engineering in Agriculture, Environment and Food, 12*, 118–125. https://doi.org/10.1016/j.eaef.2018.11.001

Upadhyay, G., & Raheman, H. (2020). Effect of velocity ratio on performance characteristics of an active-passive combination tillage implement. *Biosystems Engineering, 191*, 1–12. https://doi.org/10.1016/j.biosystemseng.2019.12.010

Usaborisut, P., & Prasertkan, K. (2018). Performance of combined tillage tool operating under four different linkage configurations. *Soil and Tillage Research, 183*, 109–114. https://doi.org/10.1016/j.still.2018.06.004

Usaborisut, P., & Prasertkan, K. (2019). Specific energy requirements and soil pulverization of a combined tillage implement. *Heliyon, 5*, Article e02757. https://doi.org/10.1016/j.heliyon.2019.e02757

Weise, G. (1993). Active and passive elements of a combined tillage machine: Interaction, draught requirement and energy consumption. *Journal of Agricultural Engineering Research, 56*, 287–299. https://doi.org/10.1006/jaer.1993.1080